European Journal of Pharmaceutics and Biopharmaceutics 132 (2018) 94–102

Contents lists available at ScienceDirect

European Journal of Pharmaceutics and Biopharmaceutics

journal homepage: www.elsevier.com/locate/ejpb

Research paper

S-Nitrosoglutathione loaded poly(lactic-co-glycolic acid) microparticles for prolonged nitric oxide release and enhanced healing of methicillin-resistant *Staphylococcus aureus*-infected wounds

Shwe Phyu Hlaing[a,1], Jihyun Kim[a,b,1], Juho Lee[a], Nurhasni Hasan[a], Jiafu Cao[a], Muhammad Naeem[a], Eun Hee Lee[c], Jae Ho Shin[d], Yunjin Jung[a], Bok-Leul Lee[a], Byung Hak Jhun[b], Jin-Wook Yoo[a,*]

[a] College of Pharmacy, Pusan National University, Busan, South Korea
[b] Department of Cogno-Mechatronics Engineering, College of Nanoscience & Nanotechnology, Pusan National University, Busan, South Korea
[c] College of Pharmacy, Korea University, Sejong, South Korea
[d] Department of Chemistry, Kwangwoon University, Seoul, South Korea

ARTICLE INFO

Keywords:
Nitric oxide
S-nitrosoglutathione
Poly (lactic-co-glycolic acid) microparticles
Methicillin-resistant *Staphylococcus aureus*
Wound healing

ABSTRACT

Methicillin-resistant *Staphylococcus aureus* (MRSA)-infected wounds have become a significant clinical issue worldwide. Recently, nitric oxide (NO) has emerged as a potent antibacterial agent against MRSA infections and a wound-healing enhancer. Nevertheless, clinical applications of NO have been largely restricted by its gaseous state and short half-life. In this study, our aim was to develop S-nitrosoglutathione (GSNO, an endogenous NO donor)-loaded poly(lactic-co-glycolic acid) [PLGA] microparticles (GSNO-MPs) that release NO over a prolonged period, to accelerate the healing of MRSA-infected wounds with less frequent dosing. GSNO was successfully encapsulated into PLGA microparticles by a solid-in-oil-in-water emulsion solvent evaporation method. Scanning electron microscopy and X-ray diffraction analyses confirmed the successful fabrication of GSNO-MPs. The latter released NO in a prolonged manner over 7 days and exerted a remarkable antibacterial activity against MRSA in a concentration- and time-dependent manner. Moreover, GSNO-MPs had good antibacterial efficacy and were found to accelerate wound healing in a mouse model of MRSA-infected wounds. Therefore, NO-releasing MPs devised in this study may be a promising option for the treatment of cutaneous wounds infected by drug-resistant bacteria such as MRSA.

1. Introduction

Methicillin-resistant *Staphylococcus aureus* (MRSA), which is a multidrug-resistant strain of *Staphylococcus*, has long been recognized as a major nosocomial pathogen worldwide [1–4]. Because community-acquired MRSA has been increasingly detected on the skin and mucosal membranes, MRSA infection of wound sites is one of the major causes of cutaneous-infection–related morbidity and mortality [5–7]. Surgical site infection with MRSA has been associated with a higher mortality rate than that caused by methicillin-susceptible *S. aureus* [8,9]. Considering that the increasing prevalence of MRSA in wounds despite the use of currently available antibiotics is a significant clinical issue worldwide, there is an urgent need for a new potent drug that would eradicate MRSA in the wound area and accelerate wound healing [10,11].

In recent years, nitric oxide (NO) has emerged as a potent antimicrobial and wound-healing agent. NO has important biological functions such as vasodilation and neurotransmission. It is synthesized in large quantities by inducible nitric oxide synthase upon infection [12]. NO interacts with oxygen or reactive oxygen intermediates to

Abbreviations: Blank-MPs, blank PLGA microparticles; CFU, colony-forming unit; DCM, dichloromethane; DETA-NONOate, (Z)-1-[N-(2-aminoethyl)-N-(2-ammonioethyl)amino]diazen-1-ium-1,2-diolate; FBS, fetal bovine serum; PEI/NONOate, polyethyleneimine/diazeniumdiolate; GSH, reduced glutathione; GSNO, S-nitrosoglutathione; GSNO-MPs, GSNO-loaded PLGA microparticles; H&E, hematoxylin and eosin; MRSA, methicillin-resistant *Staphylococcus aureus*; MTT, thiazolyl blue tetrazolium bromide; NONOates, diazeniumdiolates; PLGA, poly(lactic-co-glycolic acid); PVA, poly(vinyl alcohol); RSNOs, S-nitrosothiols; TSB, tryptic soy broth; w/o/w, water-in-oil-in-water

* Corresponding author at: College of Pharmacy, Pusan National University, Busan 609-735, South Korea.
E-mail address: jinwook@pusan.ac.kr (J.-W. Yoo).

[1] Both authors contributed equally to this work.

https://doi.org/10.1016/j.ejpb.2018.09.009
Received 28 June 2018; Received in revised form 10 September 2018; Accepted 11 September 2018
Available online 14 September 2018
0939-6411/

form reactive oxidative and nitrosative species, which exert antibacterial action via multiple mechanisms including attacking bacterial DNA, disturbing protein synthesis, and damaging essential amino acid residues in bacterial cell membranes [13]. Unlike conventional antibiotics that have a single antibacterial mechanism, NO has not been reported to elicit bacterial resistance owing to its multiple antibacterial mechanisms [13,14]. NO also plays a pivotal role in wound-healing processes including angiogenesis, cell proliferation, and tissue remodeling [15–18].

Despite the beneficial functions in infected wounds, clinical applications of NO have been restricted by its gaseous state and short half-life (2–3 s). To overcome these limitations, various NO delivery systems involving NO donors such as diazeniumdiolates (NONOates) and S-nitrosothiols (RSNOs) have been developed to control stability, prevent a rapid release, and deliver a sufficient amount of NO to a specific site for efficient therapeutic outcomes [19–22]. NONOates have been extensively used in NO delivery systems because of the predictable NO release profile. Yoo and colleagues have fabricated DETA NONOate-loaded poly(lactic-co-glycolic acid) [PLGA] microparticles; however, the microparticles released more than 80% of loaded NO within 6 h, which is not suitable for long-term NO delivery [23]. In another study, PEI/NONOate-loaded PLGA nanoparticles released ~50% of NO within 24 h, resulting in frequent dosing (every other day) for *in vivo* applications. NO-releasing hydrophobic polymers based on NONOates synthesized from polyamine compounds also have been designed for a sustained NO release [19,24]. Nevertheless, cytotoxicity due to the formation of carcinogenic N-nitrosamine is still a problem [25,26]. RSNOs have also been popular as NO donors. In particular, S-nitrosoglutathione (GSNO) has gained much attention because it is one of the relatively stable endogenous RSNOs [27]. GSNO decomposes into GSH and GSSG, which are abundant in animal cells and are proven safe [28,29]. GSNO has been physically blended or conjugated with polymers for the controlled release of NO because it is decomposed by metal ions, enzymes, ascorbic acid, changes of temperature, and by light [30]. Water-soluble polymers such as Pluronic F-127 and chitosan have been blended with GSNO to form NO-releasing hydrogels or films for topical application [31–33]. On the other hand, a rapid NO release ranging from several to 24 h is still a limitation and requires fresh preparation and frequent application.

In this study, we hypothesized that GSNO-loaded PLGA microparticles (GSNO-MPs) can release NO over a prolonged period for the enhanced healing of MRSA-infected wounds without frequent administration. PLGA was selected as the synthetic polymer because it has been well established as a biocompatible biodegradable polymer approved by the US FDA and has long been used for development of controlled drug delivery systems [34,35]. Physicochemical properties of GSNO-MPs were characterized, and a NO release assay was performed. Antibacterial activity against MRSA was investigated, and *in vivo* wound healing activity of GSNO-MPs was evaluated in a mouse model of MRSA-infected full-thickness wounds.

2. Materials and methods

2.1. Materials

PLGA (50:50 DLG 5E) was purchased from Lakeshore Biomaterials (Birmingham, AL). Poly(vinyl alcohol) [PVA], reduced glutathione (GSH), sodium nitrite ($NaNO_2$), sodium phosphate monobasic anhydrous, and thiazolyl blue tetrazolium bromide (MTT) were bought from Sigma-Aldrich (MO, USA), and argon (Ar) gas from HANA Gas (Gimhae, Korea). Bacto™ tryptic soy broth (TSB) and agar were acquired from Becton Dickinson & Company (France), whereas fetal bovine serum (FBS) and penicillin-streptomycin from Hyclone (Thermo Fisher Scientific Inc, MA, USA). All other materials and solvents used were of the highest analytical grade.

2.2. Preparation of microparticles

GSNO was synthesized via a reaction of GSH and acidified nitrite as previously described [28,36]. Synthesized GSNO was loaded into a biodegradable polymer (PLGA) by a solid-in-oil-in-water (s/o/w) emulsion solvent evaporation method [37]. In particular, 133 mg of the PLGA polymer was dissolved in 1 mL of dichloromethane (DCM). The primary emulsion (solid-in-oil emulsion) was obtained by adding 13.3 mg of a GSNO powder into the polymer solution and by emulsification with a probe sonicator at 300 W for 60 s. Then, the primary emulsion was poured into 20 mL of a 1% PVA solution and stirred continuously at 600 rpm until all DCM evaporated and GSNO-MPs hardened. The hardened GSNO-MPs were collected by centrifuging at 115*g* for 5 min and washed three times with cold distilled water. The washed GSNO-MPs were then freeze-dried overnight and stored at −20 °C for further experiments. The blank PLGA microparticles (Blank-MPs) were also prepared by the same procedure without addition of the GSNO powder.

2.3. Measurement of GSNO loading

In an aqueous solution, GSNO has a characteristic absorption peak at 335 nm with an extinction coefficient of 922 $M^{-1} cm^{-1}$ [28,38]. Encapsulation of GSNO within GSNO-MPs was quantitatively evaluated by dissolving 5 mg of GSNO-MPs in 0.5 mL of acetonitrile first and then adding 1 mL of distilled water to dissolve GSNO. Then we evaluated the significant peak by UV–Vis spectrometry [39]. The NO donor–loading capacity was calculated as the ratio of the amount of GSNO encapsulated in GSNO-MPs to the amount of microparticles. Additionally, encapsulation efficiency was calculated as the ratio of the actual to theoretical loading based on the total amount of GSNO in the procedure.

2.4. Characterization of the microparticles

The surface morphology of microparticles was investigated by scanning electron microscopy (SEM) under an FE-SEM S4800 microscope (Hitachi Ltd., Tokyo, Japan) at the accelerating voltage 10 kV. Briefly, a small amount of microparticles was mounted on a double-sided carbon tape and coated with platinum for 2 min in vacuum. For cross-sectional images, before coating with platinum, the microparticles were cut with a razor blade. The X-ray diffraction patterns of the GSNO powder, Blank-MPs, GSNO-MPs, and dissolved GSNO-MPs in DCM (GSNO extracted from GSNO-MPs) were determined by means of D8 ADVANCE with Davinci (Bruker AXS Inc., GmbH, Germany). The size of MPs was assessed by measuring at least 100 particles of each batch in the ImageJ software (National Institutes of Health, Bethesda, MA, USA).

2.5. In vitro NO release

The NO release pattern of GSNO-MPs was analyzed directly by a chemiluminescence method (Sievers NOA 280i, GE Analytical Instruments, Boulder, Co., USA). To be precise, 50 mg of GSNO-MPs was added into an incubation glass bulb, which was filled with 60 mL of a releasing medium (1 × phosphate-buffer saline; PBS) at pH 7.4 preheated to 37 °C in a water bath. The NO that was released from GSNO-MPs was carried by a continuously flowing stream of inert gas (argon) into the NOA system that had been pre-calibrated. The real-time NO release levels in ppb unit were monitored every five seconds. The percentage of the NO release at a specific time point was calculated as the ratio of the amount of an NO release at a specific time point to the total amount of NO released.

2.6. In vitro antibacterial activity

In this assay, gram-positive MRSA was used. TSB agar plates and

TSB broth were employed for growing bacteria and for colony-forming unit (CFU)-based measurement of bacterial viability. The bacteria were cultured in TSB broth at 37 °C in a shaking incubator at 100 rpm for 15 h. The resulting bacterial suspension was washed with 0.85% NaCl twice to remove the remaining medium by centrifugation at 4000*g* for 10 min. The supernatant was discarded, and bacterial pellets were re-suspended in 1× PBS to an appropriate concentration (10^8 CFU/mL) for an *in vitro* antibacterial test. Different final concentrations of GSNO-MPs (0, 12.5, 50, 100, and 200 mg/mL) were incubated with the prepared bacterial suspension. As a control, a bacterial suspension in PBS and the same amount of Blank-MPs were incubated. All tubes with the MPs and bacterial suspension were incubated at 37 °C for 24 h in a shaking incubator. For a bacterial viability assay, the incubated bacterial solutions were serially diluted (10^{-1} to 10^{-10}), and 100 µL of each dilution was spread on TSB agar plates. The agar plates were incubated at 37 °C overnight and then the colonies on the agar plates were counted to confirm bacterial viability.

2.7. In vitro cytotoxicity study

Since GSNO is known to be toxic in high concentrations, we tested the cytotoxicity of GSNO-MPs in fibroblast cells. Cytotoxicity of the microparticles and free GSNO was evaluated by using L929 mouse fibroblast cells. L929 cell line obtained from KCLB (Seoul, South Korea) were cultured in DMEM/High glucose medium (HyClone Laboratories, Logan, Utah) which was supplemented with 10% (v/v) fetal bovine serum, 100 IU/mL penicillin G sodium, and 100 µg/mL streptomycin. The cells were grown in an incubator with a humidified atmosphere of 5% CO_2 at 37 °C (Sanyo, MCO-18AIC, Japan). Cells were seeded in 96-well plates at the concentration 5×10^4 cells/well and were incubated in the incubator for 24 h. The medium was changed and cells were treated with new medium containing various GSNO concentrations 1.25, 2.5 and 5 mg/mL and incubated for 24 h in the CO_2 incubator. Floating cells and remaining microparticles were washed with sterilized PBS for three times. Sterile MTT reagent was added according to the protocol and incubated for 1 h. The MTT reagent was removed and added 100 µL DMSO to solubilize insoluble crystals of MTT formazan. The intensity of absorbance was measured at 540 nm by microplate reader. Cells incubated in medium were used as a control. The cell viability was calculated as the ratio of the absorbance of treated cells to the absorbance of controlled cells.

2.8. In vivo MRSA-infected wound healing

Animal experiments were conducted in accordance with the regulations of Pusan National University and Korean Legislation on animal studies. Male ICR mice (7 weeks of age) weighing 30–35 g were chosen as the animal model. Animals were provided food and water and kept at 25 ± 3 °C on a 12 h light/dark cycle. Avertin was injected intraperitoneally to anesthetize the mice before creation of wounds in the dorsal area. Briefly, the dorsal hair of mice was removed by an electric razor, and two bilateral skin pieces were excised with a biopsy punch (8 mm) to create full-thickness wounds. The wounds were cleaned with 75% ethanol, which was then allowed to evaporate. Then, wounds were infected with 10 µL of a prepared MRSA solution (4×10^8 CFU/mL) and covered with a Tegaderm® film overnight to establish infected wounds. The next day, the mice were chosen randomly and arranged into three groups with seven mice in each group: a control (untreated), Blank-MP, and GSNO-MP groups. Every 4 days, 10 mg of GSNO-MPs or Blank-MPs was topically applied, and photographs of the wounds were taken (Days 1, 5, 9, and 13). Each wound was covered with Tegaderm® film (including untreated mice), secured with cotton gauze, and tied with a tape. Digital images of the wounds were captured using a digital camera to evaluate macroscopic changes in the wounds. The wound size reduction (%) was determined in the ImageJ software and calculated as the percentage ratio of the wound area at a specific time point to the wound area on the first day of drug application.

2.9. Histological analysis of the MRSA-infected wound area

On Day 13, animals were euthanized, and full-thickness wound specimens were collected for histological analysis. The collected skin samples were fixed in formalin for 24 h and then embedded in paraffin. The paraffin-embedded blocks were cut vertically at 5-µm thickness on a microtome and fixed on glass slides; they were then stained with hematoxylin and eosin (H&E) and Masson's Trichrome. The stained skin histological slides were examined by light microscopy (Olympus CX40), and images were captured to observe morphology and collagen deposition in the wound area.

2.10. Bacterial burden in the wounds

The wound tissue samples collected on the last day of the animal experiment (described in Section 2.9) were stained with Twort's Gram stain to visually examine bacterial viability in the wound area. In addition, bacterial viability at wound sites was evaluated by excising the wound skin area with an 8 mm biopsy punch, by chopping this sample, and homogenizing it in sterilized PBS (1 mL). After serial dilutions (1:10), 100 µL of wound homogenates was plated on a TSB agar plate and incubated at 37 °C overnight. The bacterial viability was determined by counting the colonies (CFU/cm^2) forming on the agar plates.

2.11. Statistical analysis

Data were expressed as mean ± SD. Statistical analyses of all *in vitro* and *in vivo* data were performed by two-way ANOVA and one-way ANOVA followed by Bonferroni's test in GraphPad Prism 5.0 (GraphPad Software, Inc., LA Jolla, CA, USA). Data with P values < 0.001 were considered statistically significant.

3. Results and discussion

3.1. Fabrication of GSNO-MPs

Given that GSNO is highly hydrophilic and unstable in a hydrated state, we prepared GSNO-loaded MPs by various emulsion methods to find an optimal fabrication method. First, we attempted the most widely used double-emulsion method: the water-in-oil-in-water (w/o/w) solvent evaporation method. Although the whole process was carried out under cold conditions with protection from light to reduce degradation of aqueous GSNO, the loading capacity was lower than 1%. This result can be explained by the high hydrophilicity of GSNO; this property causes diffusion from the inner oil phase to the external water phase. Second, we tried the water-in-oil-in-oil (w/o/o) solvent evaporation method to prevent the release of hydrophilic encapsulated aqueous GSNO. Particles with a diameter less than 100 µm were obtained; however, the amount of loaded GSNO was too small to be detected. Finally, we encapsulated a GSNO powder to reduce degradation and loss of GSNO, which is unstable in the aqueous phase during encapsulation and solvent evaporation. The whole process is similar to the w/o/w method, except the GSNO powder was dispersed in a PLGA solution (oil phase) by a homogenizer. This action resulted in increased loading capacity: up to ~3%. We optimized the fabrication method by sonicating the primary emulsion (the GSNO powder in the PLGA solution); this approach can not only disperse but also reduce the size of GSNO particles in the PLGA solution. In addition, solvent evaporation duration was reduced to prevent the loss of GSNO into the external water phase; however, it took some time for GSNO-MPs to become sufficiently hard. Because loading capacity and particle size can be affected by various parameters like polymer concentration, sonication power, and stirring speed, we formulated different drug:polymer ratios

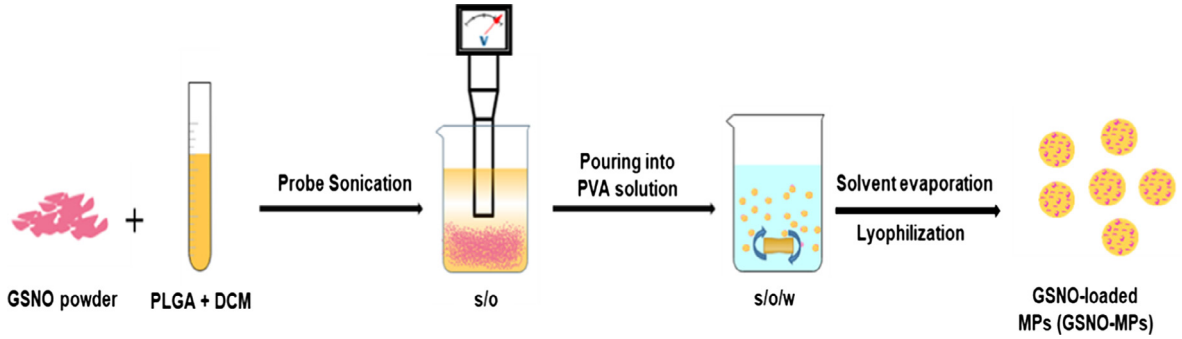

Fig. 1. Schematic illustration of fabrication of GSNO-MPs.

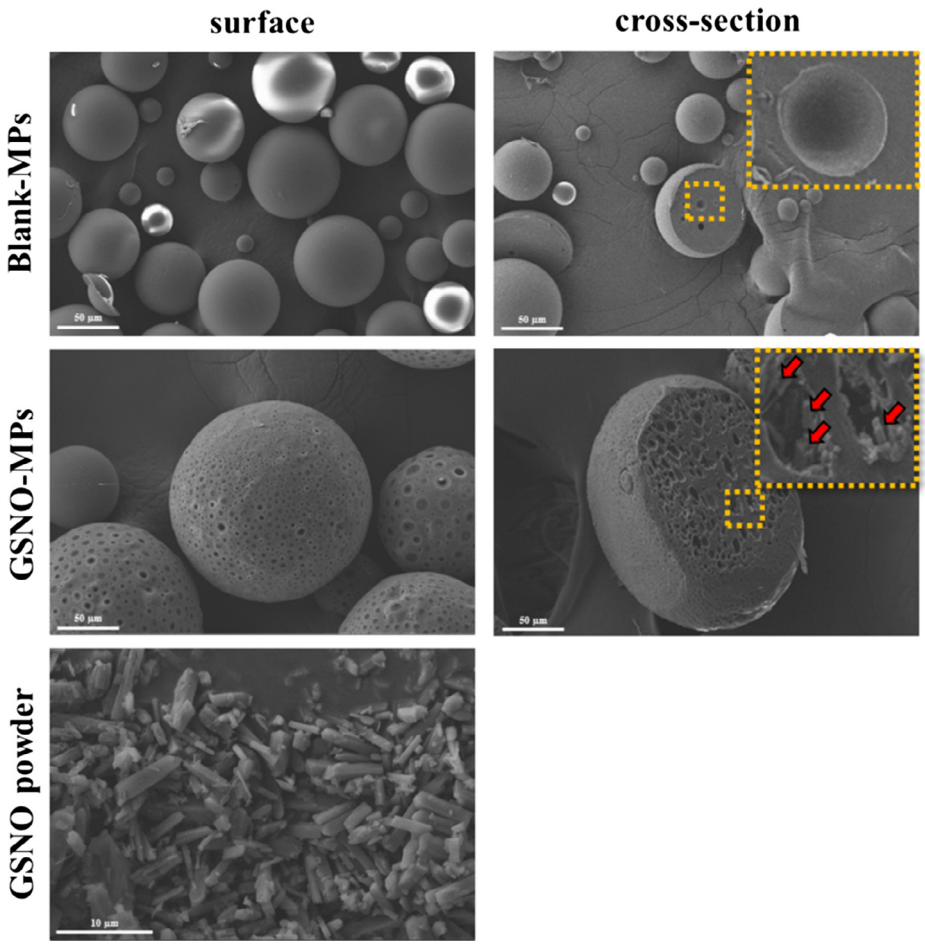

Fig. 2. SEM images of the surface and cross-sections of Blank-MPs, GSNO-MPs, and a GSNO powder. Red arrows indicate GSNO particles inside GSNO-MPs. Scale bar = 10.0 µm. (For interpretation of the references to colour in this figure legend, the reader is referred to the web version of this article.)

(1:1, 1:3, 1:5, 1:7, and 1:10) to increase the encapsulation efficiency (%). Increasing the amount of GSNO in a formulation with a fixed polymer concentration did not have any effect on encapsulation efficiency. Nonetheless, the concentration of the polymer solution affected not only particle size but also loading capacity. A higher polymer concentration resulted in larger particle size and higher loading capacity. On the other hand, when the particle size was larger than 200 µm, particles with a wider size distribution were formed and aggregated. Therefore, we chose the current particle size of GSNO-MPs (~150 µm), which helps to encapsulate maximum 5% (w/w) of GSNO at encapsulation efficiency 57.6% ± 6.5% (mean ± SD) for further study. Finally, slightly pink GSNO-MPs were successfully fabricated by the optimized s/o/w emulsion solvent evaporation method as illustrated in Fig. 1.

3.2. Characterization of GSNO-MPs

The morphological features of the GSNO powder, Blank-MPs, and GSNO-MPs were examined by SEM (Fig. 2). Blank-MPs had a smooth surface without pores on the exterior. A cross-section of blank-MPs revealed few hollow spherical pores inside. In contrast, the surface of GSNO-MPs had numerous small pores. This phenomenon can be due to the release of gaseous NO after degradation of GSNO during particle formation before PLGA hardens. This effect also resulted in a loss of GSNO into the external water phase during encapsulation and solvent evaporation processes. Thus, the presence of pores can be attributed to the low loading capacity of GSNO-MPs. Not only the external surface but also the cross-section of GSNO-MPs contained irregularly shaped pores. Magnification of the pores inside GSNO-MPs clearly revealed

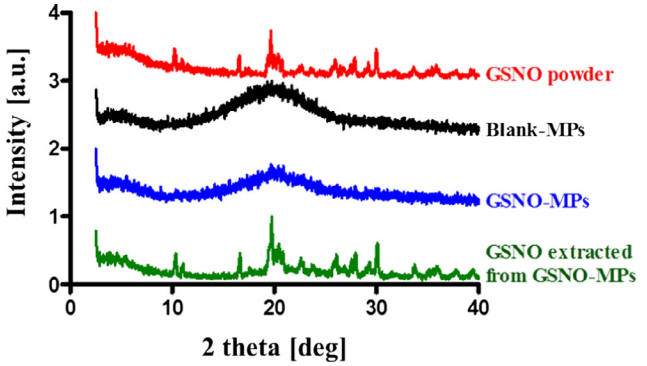

Fig. 3. The X-ray diffraction patterns of the GSNO powder, Blank-MPs, GSNO-MPs, and GSNO extracted from GSNO-MPs.

Table 1
Characterization of microparticles.

Formulation	Size (μm)	Loading capacity (%)	Encapsulation efficiency (%)
Blank-MPs	91.9 ± 10.1	–	–
GSNO-MPs	158.7 ± 20.5	5.2 ± 0.6	57.6 ± 6.5

that rod-shaped GSNO particles were encapsulated inside GSNO-MPs; this phenomenon can be confirmed by comparison with the SEM images of free GSNO powder. Therefore, encapsulation of the GSNO powder within GSNO-MPs can be visually evaluated by comparing the SEM images of GSNO-MPs and Blank-MPs. As presented in Fig. 3, the X-ray diffraction pattern revealed four significant peaks of the GSNO powder at 2 theta 10, 16, 20, and near 30. Nevertheless, in the case of Blank-MPs and GSNO-MPs, there was no significant peak, thus indicating the absence of the GSNO powder outside microparticles. When GSNO-MPs were dissolved in DCM, the peaks of GSNO appeared again, indicating the presence of GSNO inside GSNO-MPs. As shown in Table 1, the particle sizes of GSNO-MPs and Blank-MPs were 158.7 ± 20.5 and 91.9 ± 10.1 μm, respectively (mean ± SD). The larger size of GSNO-MPs can be explained by the encapsulation of the GSNO powder, which occupies space inside particles and makes them unable to shrink as do Blank-MPs during solvent evaporation. The resulting loading capacity and encapsulation efficiency of GSNO-MPs were evaluated as mentioned in the Methods section.

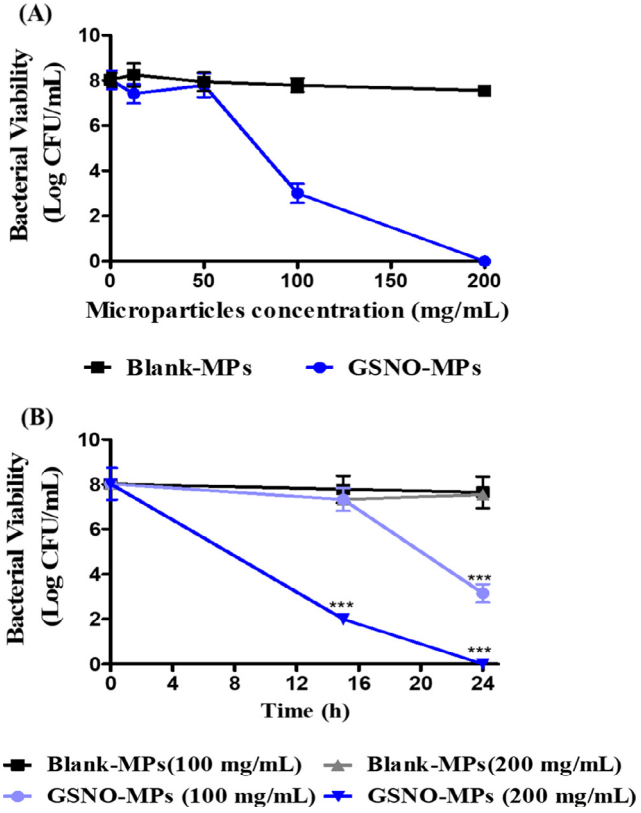

Fig. 5. Antibacterial activity of Blank-MPs and GSNO-MPs against MRSA. CFU of MRSA exposure to (A) Different concentrations of microparticles, (B) different incubation periods. Data shown are mean ± SD (n = 3), $^{***}P < 0.001$ as compared to the same concentration of Blank-MPs and incubation time.

3.3. In vitro NO release

An extended NO release is a key property of GSNO-MPs intended to achieve accelerated healing of infected wounds with less frequent

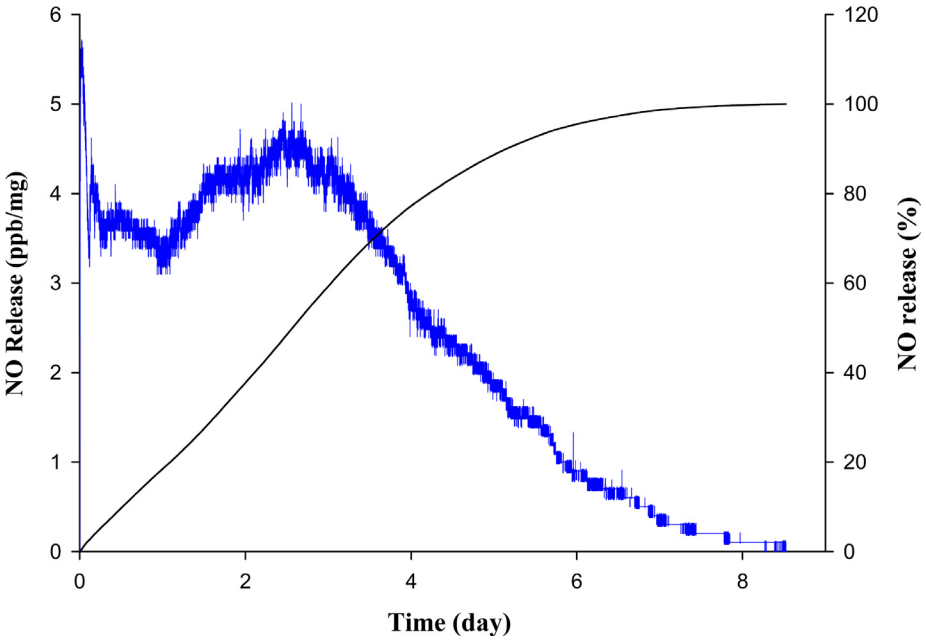

Fig. 4. Nitric oxide release profile from GSNO-MPs. Blue-colored line shows the real-time monitoring of NO release (ppb/mg) from GSNO-MPs detected every five seconds, dark-colored line shows the percentage of NO release from GSNO-MPs. (For interpretation of the references to colour in this figure legend, the reader is referred to the web version of this article.)

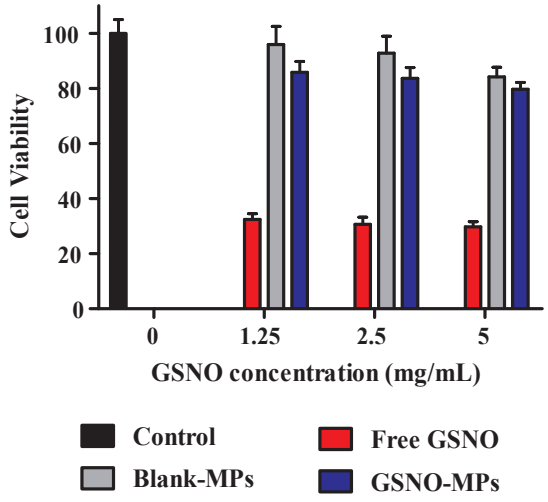

Fig. 6. *In vitro* viability of L929 fibroblast cells after incubating 24 h with microparticles at various concentrations. Data shown are mean S.D., (n = 8).

application. PLGA microparticulate systems have been used for a controlled release of drugs from several weeks to several months with a triphasic release pattern (initial burst release, lag time, and first-order release). Nonetheless, there are two major technical problems with the particulate system. First, the initial burst release can cause serious toxicity, and second, the lag phase could indicate a lack of a sufficient drug release for effective treatment [40,41]. As presented in Fig. 4, GSNO-MPs released only ~20% of NO release within 24 h and a sustained release of NO was continued for more than 7 days in the releasing medium (PBS at pH 7.4). Unlike in other studies, ~80% of total NO was released in a constantly increasing pattern for 4 days, and the remaining 20% of loaded NO was released as a lag phase. To avoid the lack of a sufficient drug release, 96 h is assumed as the therapeutic duration of GSNO-MPs and was employed in further *in vivo* experiments.

3.4. Antibacterial activity

The antibacterial activity of GSNO-MPs against MRSA was studied by counting CFUs on agar plates. GSNO-MPs at five concentrations (0, 12.5, 50, 100, and 200 mg/mL) were used to test antibacterial activity (Fig. 5A). GSNO-MPs concentration at 100 mg/mL in a bacterial solution yielded a > 4 log reduction of bacterial viability. Given that the antibacterial activity of GSNO-MPs depends on the concentration of NO, a more potent antibacterial activity (an 8 log reduction of bacterial viability) was observed at the GSNO-MPs concentration 200 mg/mL. These conditions resulted in the concentration-dependent antibacterial activity of GSNO-MPs. In contrast, a significant reduction of bacterial viability was not observed with Blank-MPs, suggesting that the antibacterial activity of GSNO-MPs was due only to NO, not to the PLGA polymer or the amount of microparticles.

The time-dependent antibacterial activity of GSNO-MPs was measured to evaluate the antibacterial effect of prolonged NO release. GSNO-MPs concentration of 100 mg/mL exerted no antibacterial activity during an incubation period of 15 h. In contrast, as depicted in Fig. 5B, when the incubation period was increased to 24 h, a significant antibacterial action (> 4 log reduction of bacterial viability) was observed. In addition, the antibacterial activity of GSNO-MPs at concentration 200 mg/mL was evaluated after different incubation periods (15 and 24 h), and bacterial viability manifested a 5 and 7 log decrease, respectively. Because GSNO-MPs released NO sustainably, the reduction of bacterial viability increased with the incubation time, in line

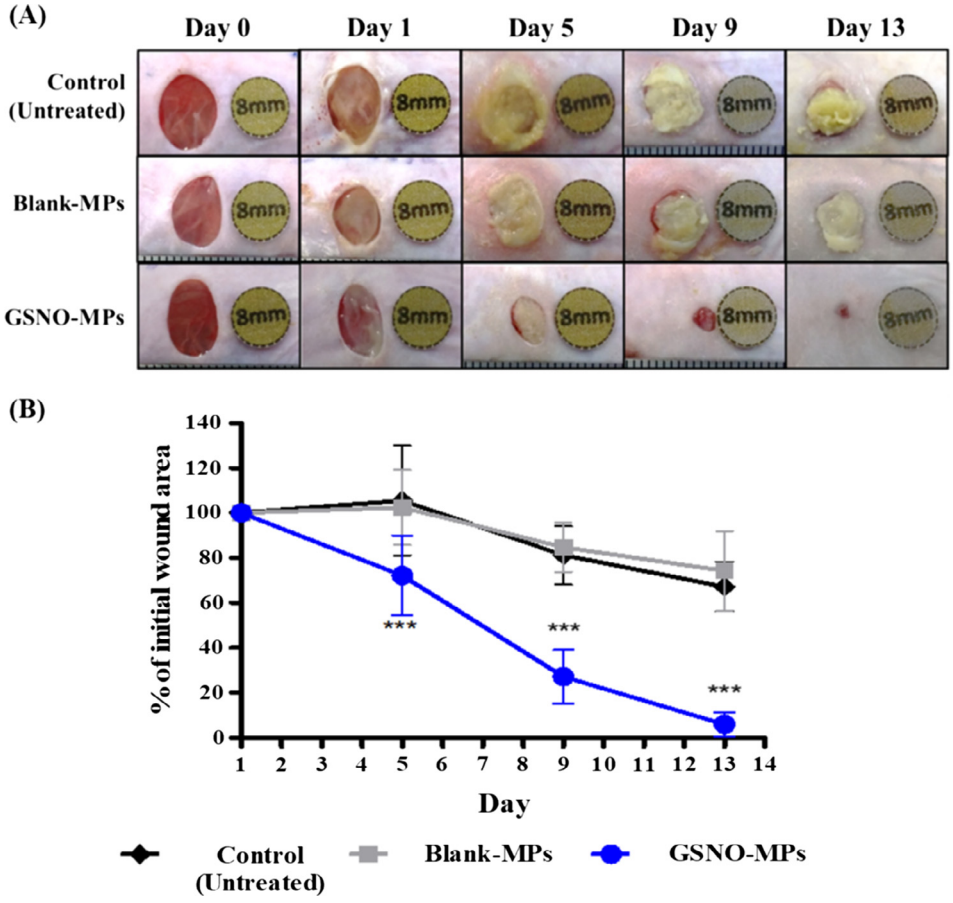

Fig. 7. Wound-healing assay in ICR mice. (A) Representative photographs of healing of MRSA-infected wounds of ICR mice treated with GSNO-MPs or Blank-MPs or untreated (control). (B) Percentage of wound area reduction. Data shown are mean ± SD (n = 8), $^{***}P < 0.001$ compared to the control (untreated group) and Blank-MPs treated group.

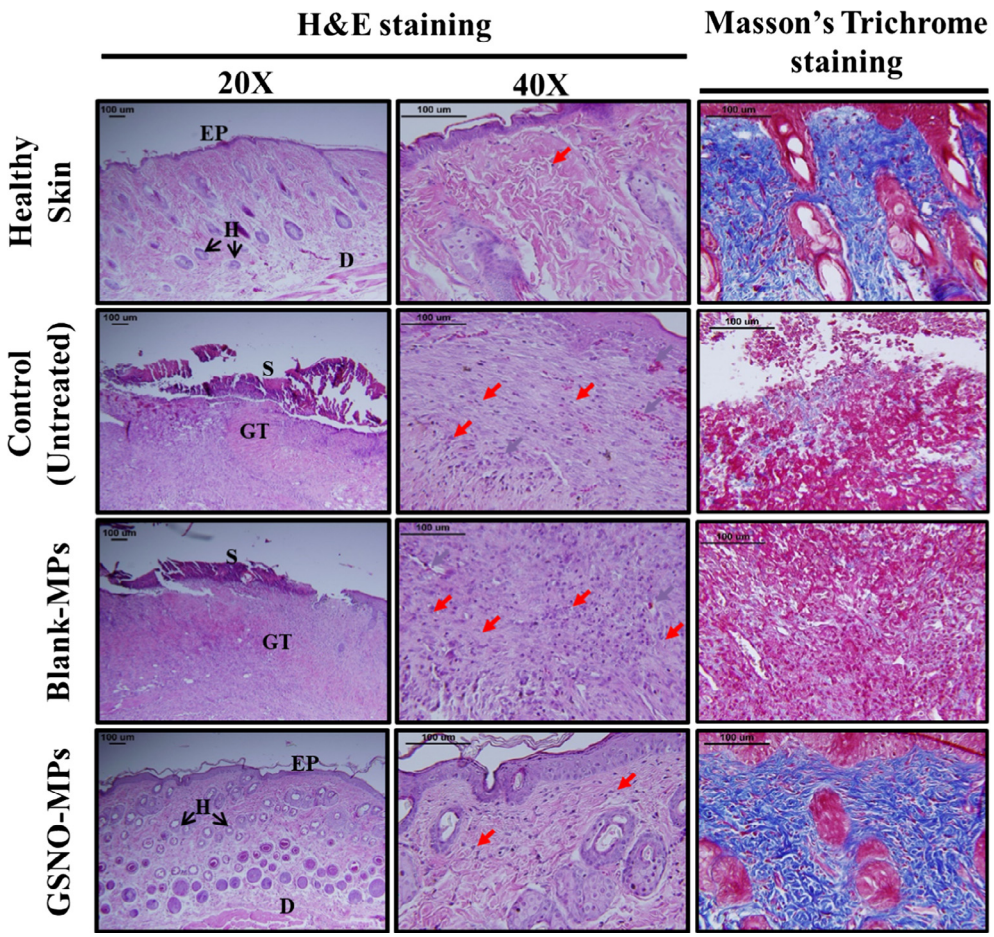

Fig. 8. Histological sections of healthy skin, untreated (control) skin, skin treated with Blank-MPs, and that treated with GSNO-MPs and stained with H&E and Masson's trichrome on Day 13. Scale bars = 100 μm. The yellow arrows indicate neovascularization, and red arrows point to inflammatory cell infiltration. EP = epidermis, H = hair follicles, GT = granulation tissue, S = wound debris, D = dermal junction. The blue color of Masson's trichrome staining denotes collagen deposition. (For interpretation of the references to colour in this figure legend, the reader is referred to the web version of this article.)

with the result of the *in vitro* release test.

3.5. In vitro cytotoxicity study

As shown in Fig. 6, free GSNO showed over 70% of cytotoxicity at the concentration of 1.25, 2.5 and 5 mg/mL whereas GSNO-MPs did not show a significant cytotoxicity (over 80% of cell viability) up to 5 mg/mL, indicating that cytotoxicity activity of GSNO can be suppressed by the micropartcile formulation. The inhibition of GSNO cytotoxicity in GSNO-MPs can be explained by the release pattern of NO from GSNO-MPs. As shown in Fig. 4, GSNO-MPs release NO over 7 days in a sustained manner, thus protecting the cells from the exposure of a high amount of NO.

3.6. Wound-healing activity

This activity was evaluated in a mouse model of MRSA-infected full-thickness wounds to test whether GSNO-MPs can eradicate MRSA in the wounds, followed by acceleration of the wound healing process thereafter. Full-thickness wounds prepared on the back of each mouse were infected with MRSA for 24 h. On Day 1, inflammation, discoloration of granulation tissue, and pocketing at the base of the wound served as the signs of infection at a wound site [42]. Each infected wound was treated with 10 mg of GSNO-MPs topically, then the dressing was changed and the drug was reapplied every 4 days (on Days 1, 5, 9, and 13). Pictures of a wound taken at predetermined periods documented the wound-healing process of three groups of animals: the control (untreated), Blank-MP, and GSNO-MP. As shown in Fig. 7A, on Day 5, the size of wounds treated with GSNO-MPs decreased to 72.1% of baseline, whereas the size of wounds in groups control (untreated) and Blank-MPs increased; this effect can be due to infection and inflammation. Wound healing in the GSNO-MP group progressed on Day 13: almost all wounds healed. In contrast, wounds with the area at 67.1% and 74.2% of baseline were still present in groups control and Blank-MPs, respectively, on Day 13. Furthermore, foul odor, inflammation, and yellowish wound debris were detected in the control (untreated) and Blank-MP. This result indicated that GSNO-MPs enhanced wound-healing activity.

3.7. Histological analysis of MRSA-infected wounds

This analysis was performed to confirm the healing of wounded tissues. On Day 13, in each animal group, skin samples were excised and stained with H&E and Masson's trichrome. Fig. 8 shows the micrographs of H&E staining of healthy skin, control (untreated), and Blank-MP and GSNO-MP treated murine skin, with cytoplasm stained purple, red blood cells stained cherry red, and nuclei blue. Complete closure of the wound area was achieved in the GSNO-MPs treated group, which resembled the morphology of normal healthy skin with a thin epidermis layer, the presence of hair and sebaceous glands, and less inflammatory infiltrate. The control (untreated) and Blank-MPs treated groups showed open wounds and increased neovascularization and inflammatory-cell infiltration in granulation tissues; these signs indicated that the wound-healing process was delayed at inflammation and proliferation phases. In addition, collagen fibers were stained blue with Masson's trichrome staining, which indicates reorganization of collagen in healed skin. In contrast to groups control (untreated) and Blank-MPs, thicker and more mature collagen fibers formed in group GSNO-MPs, as indicated by blue color intensity of Masson's trichrome stain. Thus, GSNO-MPs are effective against a MRSA-infected full-thickness wound and enhance epithelialization and collagen deposition, as commonly observed in normal healthy murine skin.

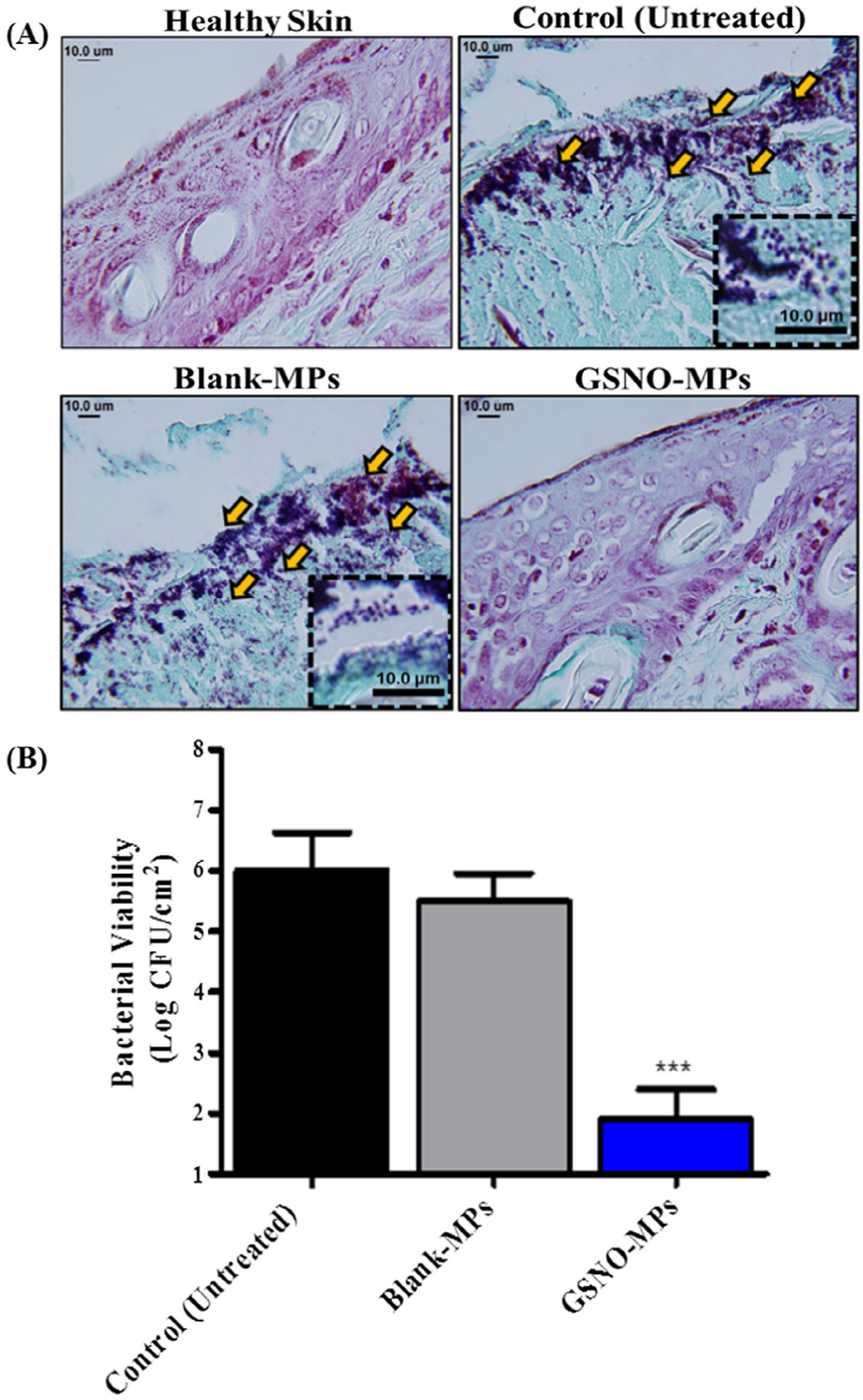

Fig. 9. Bacterial burden in the wounds at Day 13. (A) Twort's Gram staining of the skin tissue. Dark blue color spot marked with arrows indicate MRSA colonies; insets represent planktonic bacteria (cocci-shaped MRSA cells). Scale bar = 10 µm. (B) Viability of MRSA in the wounds determined by using CFU method. $^{***}P < 0.001$ compared to the control (untreated group) and Blank-MPs treated group. (For interpretation of the references to colour in this figure legend, the reader is referred to the web version of this article.)

3.8. Bacterial burden in the wounds

Whether wound bacteria remain in the wounded tissues was examined by Twort's Gram staining to confirm *in vivo* antibacterial activity. As depicted in Fig. 9A, MRSA (spherical dark blue color) was observed in the wound area of groups control (untreated) and Blank-MPs, whereas nearly no MRSA was detected in the GSNO-MPs treated group, thus confirming the antibacterial activity. To corroborate this result, the viability of bacteria in the wound area on Day 13 was evaluated by counting CFUs on agar plates (Fig. 9B). In comparison with the control (untreated) and Blank-MPs treated groups, GSNO-MPs caused a significant reduction in bacterial viability (4 log reduction), in agreement with the results on the *in vitro* antibacterial study. Thus, GSNO-MPs have antibacterial activity and can eradicate MRSA from

wounds not only *in vitro* but also *in vivo*.

4. Conclusion

In this study, GSNO-MPs were successfully fabricated by encapsulation of a GSNO powder within PLGA microparticles. GSNO-MPs showed a remarkably prolonged release NO pattern: over 7 days. Additionally, GSNO-MPs significantly decreased the viability of multi-drug-resistant MRSA. Furthermore, less frequent application of GSNO-MPs effectively enhanced wound healing in a mouse model of MRSA-infected full-thickness wounds. Therefore, the delivery system with a sustained NO release prepared in this study may be a promising approach to wound treatment under complicated conditions like infections with drug-resistant strains.

Acknowledgement

This work was supported by the Korean Healthcare Technology R& D Project, the Ministry for Health and Welfare Affairs, Republic of Korea [grant number HI15C2558].

References

[1] S.E. Cosgrove, Y. Qi, K.S. Kaye, S. Harbarth, A.W. Karchmer, Y. Carmeli, The impact of methicillin resistance in Staphylococcus aureus bacteremia on patient outcomes: mortality, length of stay, and hospital charges, Infect. Control Hosp. Epidemiol. 26 (2005) 166–174.
[2] F.D. Lowy, Antimicrobial resistance: the example of Staphylococcus aureus, J. Clin. Investig. 111 (2003) 1265–1273.
[3] R.M. Klevens, M.A. Morrison, J. Nadle, S. Petit, K. Gershman, S. Ray, L.H. Harrison, R. Lynfield, G. Dumyati, J.M. Townes, Invasive methicillin-resistant Staphylococcus aureus infections in the United States, JAMA 298 (2007) 1763–1771.
[4] R.A. Weinstein, Nosocomial infection update, Emerg. Infect. Dis. 4 (1998) 416.
[5] S.E. Cosgrove, G. Sakoulas, E.N. Perencevich, M.J. Schwaber, A.W. Karchmer, Y. Carmeli, Comparison of mortality associated with methicillin-resistant and methicillin-susceptible Staphylococcus aureus bacteremia: a meta-analysis, Clin. Infect. Dis. 36 (2003) 53–59.
[6] K. Estes, Methicillin-resistant Staphylococcus aureus skin and soft tissue infections, Crit. Care Nurs. Quart. 34 (2011) 101–109.
[7] B.A. Lipsky, Y. Tabak, R. Johannes, L. Vo, L. Hyde, J. Weigelt, Skin and soft tissue infections in hospitalised patients with diabetes: culture isolates and risk factors associated with mortality, length of stay and cost, Diabetologia 53 (2010) 914–923.
[8] J.D. Siegel, E. Rhinehart, M. Jackson, L. Chiarello, Management of multidrug-resistant organisms in health care settings, Am. J. Infect. Control 35 (2007) (2006) S165–S193.
[9] R. Köck, K. Becker, B. Cookson, J. van Gemert-Pijnen, S. Harbarth, J. Kluytmans, M. Mielke, G. Peters, R. Skov, M. Struelens, Methicillin-resistant Staphylococcus aureus (MRSA): burden of disease and control challenges in Europe, Eurosurveillance 15 (2010) 19688.
[10] G.K. Siberry, T. Tekle, K. Carroll, J. Dick, Failure of clindamycin treatment of methicillin-resistant Staphylococcus aureus expressing inducible clindamycin resistance in vitro, Clin. Infect. Dis. 37 (2003) 1257–1260.
[11] K. Hiramatsu, H. Hanaki, T. Ino, K. Yabuta, T. Oguri, F. Tenover, Methicillin-resistant Staphylococcus aureus clinical strain with reduced vancomycin susceptibility, J. Antimicrob. Chemother. 40 (1997) 135–136.
[12] C.F. Nathan, J.B. Hibbs, Role of nitric oxide synthesis in macrophage antimicrobial activity, Curr. Opin. Immunol. 3 (1991) 65–70.
[13] M.L. Jones, J.G. Ganopolsky, A. Labbé, C. Wahl, S. Prakash, Antimicrobial properties of nitric oxide and its application in antimicrobial formulations and medical devices, Appl. Microbiol. Biotechnol. 88 (2010) 401–407.
[14] C.W. Stratton, Dead bugs don't mutate: Susceptibility issues in the emergence of bacterial resistance, Emerg. Infect. Dis. 9 (2003) 10–16.
[15] S. Sortino, S. Petralia, G. Compagnini, S. Conoci, G. Condorelli, Light-controlled nitric oxide generation from a novel self-assembled monolayer on a gold surface, Angew. Chem. Int. Ed. 41 (2002) 1914–1917.
[16] J.L. Wallace, Nitric oxide as a regulator of inflammatory processes, Mem. Inst. Oswaldo Cruz 100 (2005) 5–9.
[17] S.J. Leibovich, P.J. Polverini, T.W. Fong, L.A. Harlow, A.E. Koch, Production of angiogenic activity by human monocytes requires an L-arginine/nitric oxide-synthase-dependent effector mechanism, Proc. Natl. Acad. Sci. 91 (1994) 4190–4194.
[18] M.R. Schäffer, U. Tantry, S.S. Gross, H.L. Wasserkrug, A. Barbul, Nitric oxide regulates wound healing, J. Surg. Res. 63 (1996) 237–240.
[19] M.M. Reynolds, M.C. Frost, M.E. Meyerhoff, Nitric oxide-releasing hydrophobic polymers: preparation, characterization, and potential biomedical applications, Free Radical Biol. Med. 37 (2004) 926–936.
[20] X. Zhou, J. Zhang, G. Feng, J. Shen, D. Kong, Q. Zhao, Nitric oxide-releasing biomaterials for biomedical applications, Curr. Med. Chem. 23 (2016) 2579–2601.
[21] M.C. Frost, M.M. Reynolds, M.E. Meyerhoff, Polymers incorporating nitric oxide releasing/generating substances for improved biocompatibility of blood-contacting medical devices, Biomaterials 26 (2005) 1685–1693.
[22] E.M. Hetrick, M.H. Schoenfisch, Reducing implant-related infections: active release strategies, Chem. Soc. Rev. 35 (2006) 780–789.
[23] J.W. Yoo, J.S. Lee, C.H. Lee, Characterization of nitric oxide-releasing microparticles for the mucosal delivery, J. Biomed. Mater. Res. Part A 92 (2010) 1233–1243.
[24] D.J. Smith, D. Chakravarthy, S. Pulfer, M.L. Simmons, J.A. Hrabie, M.L. Citro, J.E. Saavedra, K.M. Davies, T.C. Hutsell, D.L. Mooradian, Nitric oxide-releasing polymers containing the [N (O) NO]-group, J. Med. Chem. 39 (1996) 1148–1156.
[25] M. Miller, I. Megson, Recent developments in nitric oxide donor drugs, Br. J. Pharmacol. 151 (2007) 305–321.
[26] P.N. Coneski, M.H. Schoenfisch, Competitive formation of N-diazeniumdiolates and N-nitrosamines via anaerobic reactions of polyamines with nitric oxide, Org. Lett. 11 (2009) 5462–5465.
[27] Y. Li, P.I. Lee, Controlled nitric oxide delivery platform based on S-nitrosothiol conjugated interpolymer complexes for diabetic wound healing, Mol. Pharm. 7 (2010) 254–266.
[28] K.A. Broniowska, A.R. Diers, N. Hogg, S-nitrosoglutathione, Biochim Biophys. Acta 1830 (2013) 3173–3181.
[29] G. Wu, Y.-Z. Fang, S. Yang, J.R. Lupton, N.D. Turner, Glutathione metabolism and its implications for health, J. Nutrit. 134 (2004) 489–492.
[30] A.-S.D. Haitham, A. Ferro, S-Nitrosothiols: a class of nitric oxide-donor drugs, Clin. Sci. 98 (2000) 507–520.
[31] J. Georgii, T. Amadeu, A. Seabra, M. de Oliveira, A. Monte-Alto-Costa, Topical S-nitrosoglutathione-releasing hydrogel improves healing of rat ischaemic wounds, J. Tissue Eng. Regener. Med. 5 (2011) 612–619.
[32] T.P. Amadeu, A.B. Seabra, M.G. De Oliveira, A.M. Costa, S-nitrosoglutathione-containing hydrogel accelerates rat cutaneous wound repair, J. Eur. Acad. Dermatol. Venereol. 21 (2007) 629–637.
[33] J.O. Kim, J.-K. Noh, R.K. Thapa, N. Hasan, M. Choi, J.H. Kim, J.-H. Lee, S.K. Ku, J.-W. Yoo, Nitric oxide-releasing chitosan film for enhanced antibacterial and in vivo wound-healing efficacy, Int. J. Biol. Macromol. 79 (2015) 217–225.
[34] H.K. Makadia, S.J. Siegel, Poly lactic-co-glycolic acid (PLGA) as biodegradable controlled drug delivery carrier, Polymers 3 (2011) 1377–1397.
[35] J.M. Anderson, M.S. Shive, Biodegradation and biocompatibility of PLA and PLGA microspheres, Adv. Drug Deliv. Rev. 64 (2012) 72–82.
[36] M. Parent, F. Dahboul, R. Schneider, I. Clarot, P. Maincent, P. Leroy, A. Boudier, A complete physicochemical identity card of S-nitrosoglutathione, Curr. Pharm. Anal. 9 (2013) 31–42.
[37] G. Lautner, M.E. Meyerhoff, S.P. Schwendeman, Biodegradable poly (lactic-co-glycolic acid) microspheres loaded with S-nitroso-N-acetyl-D-penicillamine for controlled nitric oxide delivery, J. Control. Release 225 (2016) 133–139.
[38] I. Hornyák, E. Pankotai, L. Kiss, Z. Lacza, Current developments in the therapeutic potential of S-nitrosoglutathione, an endogenous NO-donor molecule, Curr. Pharm. Biotechnol. 12 (2011) 1368–1374.
[39] L.-P. Yap, H. Sancheti, M.D. Ybanez, J. Garcia, E. Cadenas, D. Han, Determination of GSH, GSSG, and GSNO using HPLC with electrochemical detection, Methods in Enzymology, Elsevier, 2010, pp. 137–147.
[40] J. Wang, B.M. Wang, S.P. Schwendeman, Characterization of the initial burst release of a model peptide from poly (D, L-lactide-co-glycolide) microspheres, J. Control. Release 82 (2002) 289–307.
[41] B. Gu, X. Sun, F. Papadimitrakopoulos, D.J. Burgess, Seeing is believing, PLGA microsphere degradation revealed in PLGA microsphere/PVA hydrogel composites, J. Control. Release 228 (2016) 170–178.
[42] S.E. Gardner, R.A. Frantz, B.N. Doebbeling, The validity of the clinical signs and symptoms used to identify localized chronic wound infection, Wound Repair Regenerat. 9 (2001) 178–186.